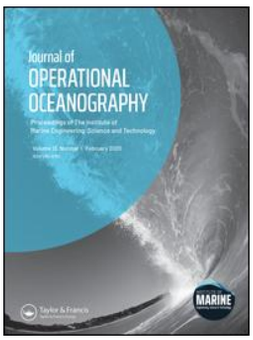

Journal of Operational Oceanography

ISSN: (Print) (Online) Journal homepage: https://www.tandfonline.com/loi/tjoo20

Assessment of Coringa Mangrove shoreline migration using geospatial techniques

Garima Sharma & K.V.K.R.K. Patnaik

To cite this article: Garima Sharma & K.V.K.R.K. Patnaik (2020): Assessment of Coringa Mangrove shoreline migration using geospatial techniques, Journal of Operational Oceanography

To link to this article: https://doi.org/10.1080/1755876X.2020.1840245

Published online: 06 Nov 2020.

JOURNAL OF OPERATIONAL OCEANOGRAPHY
https://doi.org/10.1080/1755876X.2020.1840245

Assessment of Coringa Mangrove shoreline migration using geospatial techniques

Garima Sharma and K.V.K.R.K. Patnaik

School of Naval Architecture and Ocean Engineering, Indian Maritime University, Visakhapatnam, India

ABSTRACT

Coringa Mangroves in the Kakinada Bay have evolved as the second-largest mangroves in the East Coast of India over the last century. The Coringa Mangrove shoreline has accreted considerably in the past decades as observed from the satellite imageries, adding value to the natural biodiversity of flora and fauna. This study is focused on quantifying the long term changes of Coringa mangrove shoreline using the Landsat imageries for years 1977, 1988, 2000, and 2013 using the Digital Shoreline Analysis System. For a mangrove shoreline length of 20.5 km, 41 transects were cast at an interval of 500 m for calculating the change and their migration distance using three statistical methods, namely End Point Rate (EPR), Net Shoreline Movement (NSM) and Linear Regression Rate (LRR). Results showed that there was considerable growth of mangroves in the bay leading to the seaward migration of the mangrove shoreline from the year 1977–2013. The study observed the difference in the mangrove shoreline migration dynamics in the South-eastern (near the bottom of the spit) and the western part of the Kakinada Bay. The calculated average degradation rate due to erosion is $-5.19\ m.yr^{-1}$ and the average accretion rate leading to their growth is $14.83\ m.yr^{-1}$ for all transects of the 20.5 km mangrove shoreline stretch during this period. The results hold importance as they help in identifying the regions prone to mangrove degradation and enable management planning for the protection of the eroding stretch of the mangrove shoreline.

ARTICLE HISTORY
Received 29 August 2019
Accepted 8 October 2020

KEYWORDS
Mangrove shoreline; accretion; erosion; end point rate; linear regression rate; net shoreline movement

Introduction

Mangroves are the halophytic group of plants and small trees growing in the confluence of the land and sea in the brackish water acting as an important coastline feature protecting the coast from the climatic and hydrological hazards. Mangroves majorly grow in the intertidal regions of the tropical and sub-tropical climatic regions at the upper tidal flats and are the least inundated parts of estuarine regions (Pandey and Nayak 2013). Because of their sheltered nature, mudflats and mangroves accumulate large quantities of organic matter (Jickells and Rae 1997; Cook et al. 2004a; Sanders et al. 2010b). They act as a buffer between land and sea and with the help of their complex root system, protect against coastal erosion from the action of winds, waves and currents. Anthropogenic activities like deforestation, cutting of mangrove wood for foliage, land use and land cover changes for aquaculture practices; pond formations, constructions, industrial effluent discharge and human waste disposal, etc. have led to large destruction of mangrove areas. Growth and degradation of mangroves in coastal areas are also strongly affected by the natural hydrodynamic forcing like winds, waves, tidal currents, freshwater discharge, sediment availability, sedimentation and erosion, rainfall occurring in the region. Therefore it becomes crucial to analyse the mangrove shoreline changes and quantify their rates at large timescales to identify and map the erosion of vulnerable areas for better conservation and protection planning. Tran et al. (2013) used mangrove forest edge as a shoreline indicator and NDVI to delineate mangrove shoreline by distinguishing water land and mangroves.

Remote sensing and Geographical Information System help in assessing the spatial and temporal changes in the coastal areas, shoreline changes, migration of mangrove shoreline and their boundaries with the help of satellite imageries. For this Digital Shoreline Analysis System (DSAS) is one of the Arcmap tools in GIS platform that helps in the calculation of long term changes of shoreline migration and their rates. DSAS is an effective tool that helps in Historical Trend analysis for examining the present and past mangrove shoreline position measuring the changes at the casted transects from a defined baseline as it incorporates an identified attribute position at different periods (Cohen and Lara 2003; Sheik and Chandrasekar 2011; Oyedotun 2014;

CONTACT K.V.K.R.K. Patnaik patnaikrk@gmail.com

Thinh and Hens 2017). Hence, the present study aimed to integrate the available spatial information using GIS to assess the changes in the northern boundary of the mangrove cover over different periods using remote sensing data to understand the trend of accretion and erosion of the northern boundary of Coringa mangroves of Kakinada bay as it is directly exposed to hydrodynamic forcing and is hugely impacted by the action of winds, waves, tides and currents. The outcome of this study in terms of spatial and temporal patterns of growth and degradation of mangrove can help in building a proper management plan of mangroves in the area.

DSAS can be applied for both short term coastal changes analysis (days to seasons) (Brooks and Spencer 2010; Hapke et al. 2013) as well as long term (years to decades to centuries) analysis of shoreline variations (González-Villanueva et al. 2013; Thinh and Hens 2017)

Mangrove shoreline variations along different time scales have been widely analysed and quantified using multi-temporal satellite data using DSAS. End Point Rate (EPR) is the most widely used statistical parameter for studying spatial patterns of shoreline change (Thieler et al. 2009). Alemayehu et al. (2014) assessed shoreline changes in the Watamu area of Kenya using End Point Rate, Net Shoreline Movement, Weighted Linear Regression tools of the Digital Shoreline Analysis System. They reported mean shoreline changes of EPR and NSM as 0.7 $m.yr^{-1}$ and −30.3 $m.yr^{-1}$, respectively. Mary Divya Suganya et al. (2017) studied mangrove shoreline changes for Krishna and Godavari Delta with shoreline stretches of 65 and 59 km respectively, for a period of 37 years and assessed the overall erosion rate as 1.5 and 2 $m.yr^{-1}$, respectively. They attributed overall erosion of mangrove shoreline for Krishna Delta and Godavari Delta to coastal erosion, decreased sediment discharge from rivers and stated that there had been a decline in mangrove extent due to over-exploitation of natural resources and anthropogenic activities like aquaculture.

The knowledge and assessment of mangrove shoreline changes is crucial as it gives an overall review of the morphodynamic evolution of the region and identifies the areas with mangroves vulnerable to degradation leading to mangrove shoreline erosion. This study aims to assess and the changes in Coringa mangrove shoreline delineated from Landsat imageries and quantify their rate of change using statistical methods of DSAS, namely EPR, LRR and NSM.

Materials and methods

Study area

Coringa Mangroves are located in Kakinada bay at 82° 14' – 82 °22'E longitude and 16°5' – 17°N latitude in East Godavari district of Andhra Pradesh state in India (Figure 1). Kakinada Bay is a low-lying shallow region with approximately 132km^2 in area, susceptible to natural disasters like flood, storm surges, cyclones, tsunamis and surrounded by spit at the eastern side, Coringa mangroves and three tributaries of Godavari River; Gaderu, Corangi and Mattlapalem at the southern side, Coringa mangroves, Kakinada port and city at the western side. The mouth of the bay is opened to the sea on the northern side. Kakinada has a semi-arid climate with an average rainfall of 1040 mm per annum and an average temperature of 28° Celsius (deg. C). Tides are semidiurnal and tidal amplitude in the bay varies between 2.3 and 4.5 m. Prevailing winds in Kakinada are usually south-westerly for most of the year except during October-January, when they blow north-easterly. Being a large rice zone and also part of a Special Economic Zone and a proposed petroleum, chemical and petrochemical investment region, it holds great economic importance. The current direction in the area is majorly north-easterly and then south-westerly dominated by seasonal winds that drive sediment transport inside the bay. The Godavari Estuary covers an area of 62,000 ha of which dense Coringa mangrove forest extends over 6,600 ha. Various species like *Avicennia marina, A.officinalis, Excoecaria agallocha, Aegiceras corniculatum, Sonneratia apetala, Rhizophora apiculata*, etc. are found here. It was found that an area of about 1,250 ha of mangroves was destroyed by anthropogenic interference like aquaculture and tree felling (Satapathy et al. 2007). Jaya Kumar (2014) extensively studied the management of Godavari mangrove wetlands using remote sensing and GIS applications. Several studies on mangrove mapping, identification of species, sediment dynamics and circulation mixing of Kakinada Bay have been reported (Chandramohan and Nayak 1991; Jain et al. 2008; Satyanarayana et al. 2009). An intensive study on the Godavari mangroves shoreline migration is now needed.

Methods

The Landsat images were chosen for the study as they are widely available for good spatial coverage with higher resolution and provide mostly cloud-free historical images for a long period. Landsat images for years 1977, 1988, 2000 and 2013 were used to analyse decadal shoreline changes as shown in Table 1. These four years were chosen for the study to analyse the decadal progression of mangroves towards the sea. A suite of Landsat images including a Landsat Multi-

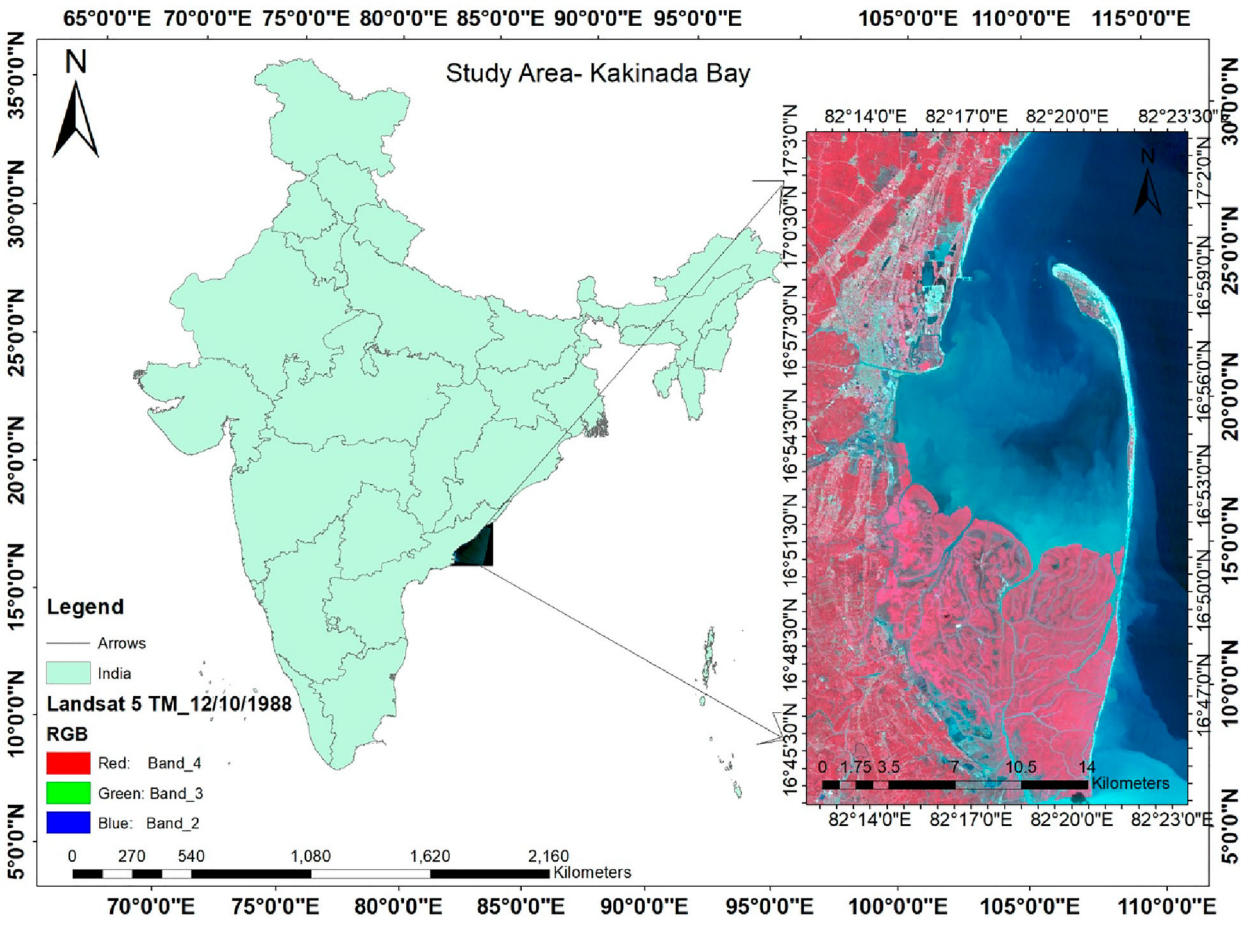

Figure 1. Map of Study area showing Coringa Mangroves and Kakinada Bay.

Spectral Scanner (MSS) data (1977), a Landsat Thematic Mapper (TM) image (1988) and a Landsat Enhanced TM Plus (ETM+) image (2000) were obtained from landsat.org. A Landsat 8 (Operational Land Imager, OLI) image (2013) was acquired from Reverb (now retired and replaced by Earthdata Search). Landsat TM data have seven spectral bands, with a spatial resolution of 30 m for bands 1–5 and 7. Landsat 8 data have nine spectral bands with a spatial resolution of 30 m for bands 1–7 and 9. Cloud cover was less than 10% for these images. All the images were obtained at a similar tidal phase to reduce tidal errors. The Landsat images were selected with acquisition time during low tide of sea level so that the maximum coastal zone gets exposed and mangrove boundaries could be determined and extracted accurately as much possible. For reducing the tide-influenced errors, the tidal conditions at the time of image acquisition were noted down as suggested by Reshma and Mani Murali (2018). Although Mangroves are evergreen and are known to be not highly different in their phenology during different times and seasons of the year as reported by Nair (2017). Most of the images were selected for the period between October to March every year as cloud-free images available during this period.

The Landsat MSS, TM and ETM+ images acquired for 1977, 1988 and 2000 were corrected for the geometric errors using the 2013 Landsat 8 (OLI) imageries as the reference image in ArcGIS. Geometric rectification is done to remove errors as remotely sensed coordinates vary from image to image due to earth's rotation and panoramic distortions during the acquisition of images (Elnabwy et al. 2020). The process removes the geometric anomalies and corrects the coordinates of images with the correct ground coordinates with the pixel location. This was carried out for each image using 10 ground control points, chosen from distinct features throughout the target image. The total root mean square error (RMSE) was below 1 pixel during the rectification of images. Resampling of the geometrically rectified images was carried out using the Cubic convolution method registering all images to the 30 m pixel size taking the year 2013 as the base image. These images were registered to the Universal Transverse Mercator

Table 1. Details of the multi-temporal satellite data products, date and time of acquisition and the tidal condition.

Satellite	Number of spectral bands	Path/Row	Acquisition date	Acquisition time	Resolution (m)	Tidal height (m)
Landsat MSS	4	*P* 152 R48	08/01/1977	04:40:00	60	0.23
Landsat 5 TM	7	*P* 141 R48	12/10/1988	04:40:00	30	0.16
Landsat 7 ETM+	8	*P* 141 R 48	08/12/2000	04:40:00	30	0.38
Landsat 8	9	*P* 141 R48	21/03/2013	04:40:00	30	0.27

system (UTM) WGS datum-1984 projection zone 44N and then subset over the study area.

Mangrove shoreline detection and Extraction

Mangrove shoreline was digitised using the seaward mangrove forest edge as the shoreline indicator. The closed-canopy forest cover was used as the border for distinguishing mangroves from the mudflats and sea (Tran et al. 2013). The normalised Difference Vegetation Index (NDVI) was used for differentiating the vegetation from the land and the sea. NDVI is considered as one of the best extensively used feature for quick and easy detection of the living green vegetation cover from other land features. The border pixels differentiating between vegetation, land and sea were delineated as mangrove shoreline.

Shoreline data analysis

To study the progression and regression rates of mangrove shoreline and its movement, the rate of change of shoreline analysis was performed in the Digital Shoreline Analysis System 4.3 (DSAS), an extension of ArcGIS developed by the USGS. DSAS computes the rate of change statistics of mangrove shoreline boundary using multiple historic shorelines in GIS with respect to the baseline position at user-specific intervals. All shorelines were compiled in the GIS geodatabase with 5 attribute fields which include Object ID (a unique number assigned to each transect), shape (polyline), shape length, ID, and date (original survey year). All shorelines were appended into a single shapefile. A baseline which is a reference datum used in the DSAS model was cast offshore and parallel to the general orientation of shorelines. It serves as a starting point to cast transects at the closest intersection using a simple baseline cast method, crossing through the individual shoreline vectors and providing measures of change over time. 41 transects were cast at 500 m length interval at right angles from a shoreline stretch of 20.5 km (Figure 2).

To calculate the accretion and erosion rates, the three most used and cited statistical methods End Point Rate (EPR), Net Shoreline Movement (NSM) and Linear Regression Rate (LRR) were employed. Net Shoreline Movement is the total distance moved by shoreline from the oldest shoreline to the youngest (Thieler et al. 2009). End Point Rate gives the rate of change of shoreline movement calculated by dividing the distance of shoreline movement by the time elapsed between the oldest and the most recent shoreline. The negative rate values indicate erosion, movement of the shoreline landwards and positive rate values indicate accretion, movement of the shoreline towards the sea. A linear regression rate-of-change statistic can be determined by fitting a least-squares regression line to all shoreline points for a particular transect. The regression line is placed so that the sum of the squared residuals (determined by squaring the offset distance of each data point from the regression line and adding the squared residuals together) is minimised. LRR is the slope of the line which indicates the meters of change per year due to erosion and mangroves degradation giving negative slope or accretion and sedimentation leading to the expansion of mangroves giving positive slope over a period of 36years.

The uncertainty of shoreline change rate was calculated by in this study determining measurement errors like rectification error (Er), digitisation error (Ed), pixel error (Ep) and positional error like a tidal error. The total uncertainty Et was calculated by taking square root of sum of the squares of each error as shown in equation 1.

$$Et = \pm\sqrt{Ep^2 + Er^2 + Ed^2 + Etd^2} \tag{1}$$

The Er rectification error is considered as the Root Mean Square Error (RMSE), Digitisation error is the error introduced while digitising shoreline on the map, pixel error is considered as the pixel size of the map and tidal error is the tidal fluctuations of shoreline calculated by using tide gauge data. The tide gauge data for each year's shoreline was assessed and the standard deviation of the tidal measurement was computed for each transect. The tidal standard deviation was calculated by the tan of a slope calculated for each transects using equation 2.

$$Etd, i = \frac{Std,\ i}{\tan\alpha,\ i} \tag{2}$$

where $Std_{,\ i}$ is the standard deviation of the vertical shoreline fluctuation and $\tan\alpha_{,\ i}$ is the section slope of

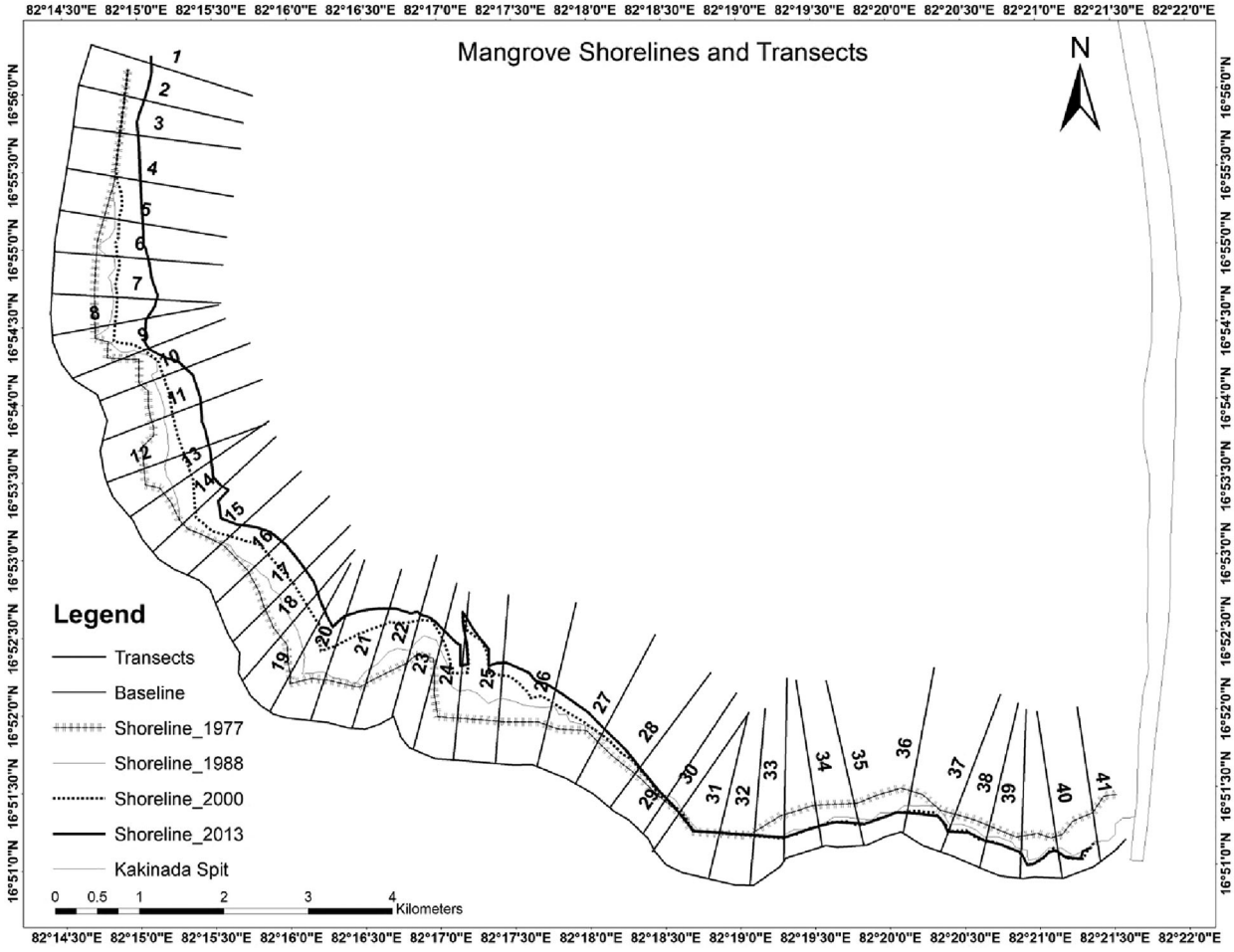

Figure 2. Mangrove Shorelines and Transects cast for the study.

the transect. Finally, the tidal error for the whole shoreline comprising of 41 transect sections was calculated by using equation 3.

$$Etd = \sqrt{(Etd,\ 1^2\ + Etd,\ 2^2 + \ldots.\ + Etd,\ n^2)/(n-1)} \tag{3}$$

The standard deviation of all transects and tidal uncertainty were computed for the shorelines for all four years (Table 2).

The shoreline change rates calculated are the regionally averaged rates measured as the average of rates of all transects of the shoreline under study assuming confidence interval on the linear regression as 95% at each transect as random and independent (Fletcher et al. 2012). Hence the uncertainty of an average rate Eavg was calculated as the root sum of squares of rate uncertainties *Ei* at all transects divided by *n* as shown in equation 4.

$$Eavg = \frac{\sqrt{\sum_{i=1}^{n} Ui^2\ )}}{n} \tag{4}$$

The average uncertainty was calculated for each year's shoreline measuring all the four kinds of errors and is summed in Table 3.

The rate of change indexes for all the shorelines End Point Rate, Linear Regression Rate and Net Shoreline Movement were evaluated for all four shorelines calculated for all 41 transects using DSAS considering the uncertainties. The statistical index results obtained were plotted with EPR, LRR in Figure 3 while NSM has shown in Figure 4 where positive values indicate accretion and negative values indicate erosion occurring in the shoreline.

Table 2. Standard Deviations *Std* of the tide fluctuations and their related tide uncertainties *Etd* for the Coringa mangrove shoreline.

Year	18 January 1977	12 December 1988	8 December 2000	21 March 2013
Std (m)	0.17	0.18	0.14	0.08
Etd (m)	0.2	0.15	0.15	0.46

Table 3. The uncertainties measured for all shoreline position (m). The total uncertainty is mentioned in bold.

Shoreline year	Rectification error	Digitisation error	Pixel error	Tidal error	Total uncertainty
1977	0.015	0.14	0.14	0.2	**0.28**
1988	0.01	0.046	0.046	0.15	**0.16**
2000	0.01	0.046	0.046	0.15	**0.16**
2013	0.009	0.042	0.042	0.46	**0.46**

Result and discussion

The overall shoreline changes were estimated from the Landsat images for period of 36 years from 1977 to 2013 using three statistical indexes EPR, LRR, NSM using DSAS. With various methodologies reported for mangrove shoreline delineation like supervised classification followed by Thinh and Hens (2017) using NDVI and mangrove forest edge as a shoreline indicator and clustering threshold technique of Otsu's classification adopted by Tran et al. (2013); this study used NDVI for digitising the seaward mangrove forest edge for delineating the mangrove shoreline. Since the Kakinada Bay is covered with mangroves at the southern bottom and the western side, mangrove shoreline was explicitly defined by NDVI for differentiating between vegetation, land and sea. The shoreline rate changes are compared for EPR and LRR. The trend differences between indices EPR and LRR has shown in Figure 3 indicate the consistent variations in the rate of accretion and erosion of the shoreline. Accretion zones are demarcated in the figure from transects 1-29. The shoreline is receding at transect 30 and from 32 to 41 transects. The average accretion rate is found to be 14.83 m.y^{-1} while the erosion rate has been found as −5.19 m.y^{-1}. Transects 30 and 31 have been relatively stable and very less shoreline change has occurred in this area with the lowest shoreline index values. The NSM trend showed in Figure 5 exhibits a similar trend with other indexes.

The End Point Rate and Linear Regression Rate presented in the above Figure 3 show that the Coringa mangrove shoreline has accreted in general over the period of 36 years. The major area accreted is at transect 24 with the end point rate at 32.88 m.y^{-1}and linear regression rate at 36.09 m.y$^{-1,}$ while the region with the least accretion is at transect 31 with end point rate at 0.34 m.y^{-1} and linear regression rate at 0.24 m.y^{-1}. End Point rate and linear regression rate with maximum erosion are at transect 33 at −7.54 m.y^{-1} and −7 m.y^{-1} respectively. The average accretion rate of EPR and LLR

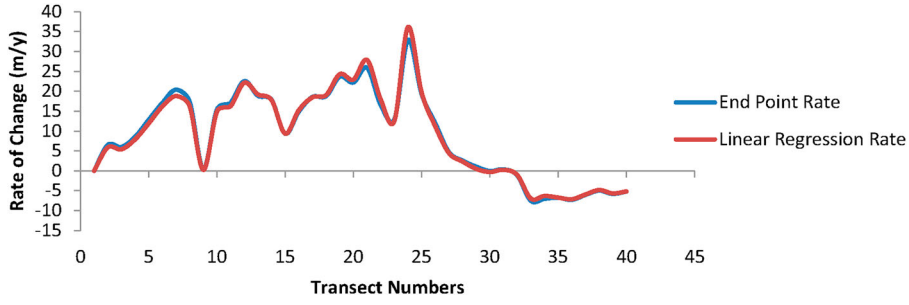

Figure 3. Comparison of the Shoreline change rate at each transect expressed by the End Point Rate (EPR) and Linear Regression Rate (LRR) for the period 1977-2013.

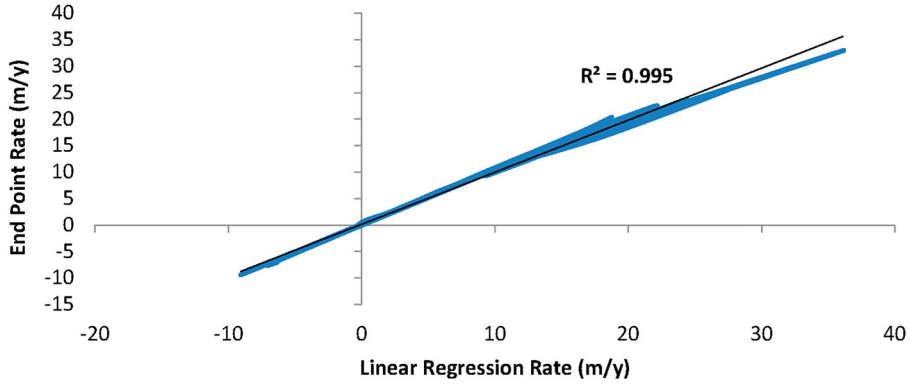

Figure 4. Comparison of shoreline change rate by two different statistical methods (End Point Rate and Linear Regression Rate).

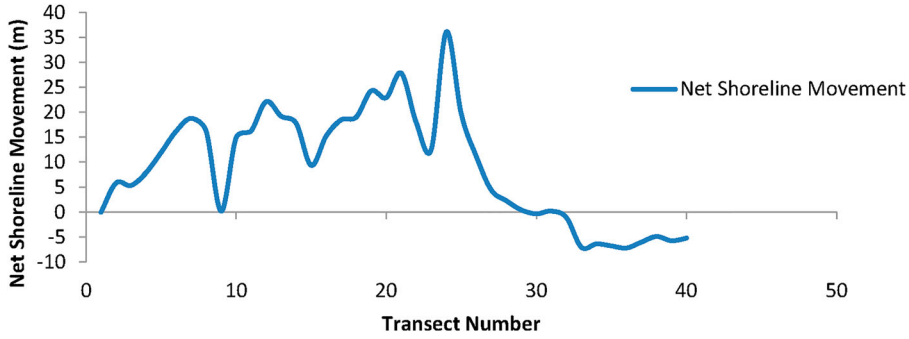

Figure 5. Shoreline change rate at each transect expressed by the Net Shoreline Movement (NSM) for the period 1977-2013.

for the whole shoreline stretch is 14.83 and 14.79 m.y^{-1} respectively while the average erosion rate of EPR and LRR is −5.19 m.y^{-1} and −5.02 m.y^{-1} respectively. Thus it has been found that there has been progradation of mangrove shoreline towards the sea for a major part of the shoreline at high shoreline change rates as shown in Table 4.

The mangrove shoreline change rate obtained by the statistical methods EPR and LRR is very similar throughout the study area. The comparison of EPR and LRR results as shown in figure 4 above presents the R-squared value for the period 1977–2013 as 0.995 which is highly correlated. The results show that the dependent and independent variables are in good correlation.

The mangrove shoreline movement in the study period has changed differently in the bay dividing it into two different zones of accretion and erosion. The results have shown the mangrove shoreline movement significantly accreting from the western side of the bay till half of the southern side of the bottom of the bay. While thereafter, the shoreline has undergone a recession for the other half of the bay bottom reaching the bottom of the spit. Mangroves have undergone significant progradation at the western side of the bay with maximum movement over transects 12 and 19 with a distance of 815.28 and 856.38 m respectively. At the southern bottom of the bay, the maximum distance accreted by mangrove shoreline is 937 and 1190.24 m at transects 22 and 25 respectively. The different behaviour of two different parts of the mangrove shoreline stretch undergoing accretion and erosion in the western and the eastern side of the bay observed in the entire period is presented in Table 5. The results indicate the hydrodynamic forcing leading to the sediment transport and deposition at the western side of the bay.

The above table shows that the mangrove shoreline stretch is significantly prograding with the high rates of shoreline accretion, while quite less shoreline stretch has receded at a very less rate of shoreline erosion.

The overall results presented in Table 5 show that there has been significant accretion in the southwest of the Bay, while there was some erosion of mangrove shoreline towards the southern end of Kakinada spit. Out of 25 transects in the western side of the bay, 24 transects have undergone accretion with the highest rate of 32.88 m.y^{-1} at transect number 24, with one transect being stable. At the south-eastern part of the bay with 15, 11 transects have undergone erosion with the maximum erosion occurred at transect 33 with an average rate −7.54 m.y^{-1}. Rest 4 transects in the south-eastern part have undergone very less accretion with the highest accretion rate of 4.68 m.y^{-1} at transect 27.

This pattern of accretion of shoreline towards the Southwest of Kakinada Bay can be attributed to the natural hydrodynamic forcing. Kakinada Bay experiences

Table 4. Overall shoreline changes from year 1977–2013.

Shoreline statistics	Erosion	Accretion
Average End Point Rate (m.y^{-1})	−5.19	14.83
Average Linear Regression Rate (m.y^{-1})	−5.02	14.79
Average Net Shoreline Movement (m)	−201	518.57

Table 5. Shoreline change rate comparison between the Western side of the bay with South-Eastern side of the bay from the year 1977-2013.

Statistics	Western Side of the bay	South-Eastern side of the bay
Mean Shoreline Change (m.y^{-1})	16.27	−3.09
Rate of Erosion (m.y^{-1})	0	−5.19
Rate of Accretion (m.y^{-1})	16.95	2.14
Maximum Rate of Erosion (m.y^{-1})	0	−7.54
Minimum Rate of Erosion (m.y^{-1})	0	−0.08
Maximum Rate of Accretion (m.y^{-1})	32.88	4.68
Minimum Rate of Accretion (m.y^{-1})	5.96	0.34
Number of Transects	25	15
Number of Transects undergoing Erosion	0	11
Number of Transects undergoing Accretion	24	4

southerly littoral currents produced by the North East monsoon waves which leads to sediment transported southwards of groins at Kakinada channel. Southerly longshore currents weaken inside the bay and with flood tide currents, fine sediments get transported towards the western side of the bay depositing at the south of the bay. Chandramohan et al. (2001) explained the process of entrapment of sediments inside the bay as tide- generated reversing flows can trap large volumes of sediments brought by flood tides and get deposited in still waters often getting trapped near jetties constructed to stabilise the entrance channel. Mudflat formation appears to be supported mainly during the monsoon season with major discharges from Gaderu and Corangi Rivers, high tidal currents and less wave energy leading to enhanced sediment discharges, especially in marshy lands which act as sediment sinks. Mudflat deposition leads to the succession of mangrove seedlings and accretion towards the sea. Slight erosion and shoreface retreat at the southeastern side of the bay suggests that sediments brought down could have been redistributed by the two currents moving in the opposite directions.

Net Shoreline Movement analysis as shown in Figure 4 indicated that out of a 20.5 km stretch of shoreline, an 15 km stretch was under accretion and a 5.5 km stretch was experiencing erosion. The accretion of sediment leads to seaward advancement of the shoreline along the southwest part of the Bay whereas loss of sediments (erosion) occurred along the southern end of the spit. Littoral cell dynamics, the geometric configuration of shorelines and associated net sediment budgets are the most important aspects that influence the spatial changes of shorelines through the times. A substantial amount of sediment loads are transferred at the Corangi and Gaderu River mouths and low wave action results in a positive net sediment budget, which results in the shoreline moving out into the sea. The shoreline transects 32–40 near the spit bottom as shown in Figure 5 comes under a negative net sediment budget, which results in the shoreline moving landward. Overall, the general trend of shoreline erosion was that it decreases eastward and becomes less near the spit.

Long term estimation of shoreline changes revealed that slight erosion of the mangrove shoreline was observed near the south of the spit, where migration was landward and amounted to a total loss of approximately 0.56 km^2. It was observed from various studies undertaken by Reddy and Roy (2008) and Murty et al. (2011) that from 1977 to 2013 total area of mangroves in the region has increased from 92 km^2 to 118.7 km^2, which can be attributed to replantation activities, natural growth and shoreline accretion. Out of the total increase in mangrove area by 26.7 km^2, accretion towards the Bay due to shoreline migration was by 18.12%. This study revealed that shoreline migration is one of the major factors contributing to the growth in the extension and increase in the mangrove region. The study attributes the respective shoreline recession and progradation to the natural hydrodynamic forcing playing a vital role in the sediment transport inside the bay. Mary Divya Suganya et al. (2017) studied the long term changes of full Godavari Delta including Kakinada bay mangrove shoreline, with a shoreline stretch of 59 km between 1972 and 2010. Their study calculated the overall accretion rate of Godavari delta to be 2.4 $m.y^{-1}$ for this period. They mentioned that there was a 7 km^2 increase in mangrove area at the southwestern part of the Kakinada Bay while erosion had occurred at the southeastern region of the Bay. Their EPR study for full Godavari Delta with a shoreline stretch of 59 km from the year 1972–2010 resulted in an overall accretion rate as 2.4 $m.y^{-1}$. While in the current study, EPR was calculated only for a 20.5 km stretch of the northern boundary of Coringa mangroves in Kakinada Bay between 1977 and 2013 which amounts to 14.83 $m.y^{-1}$ as the average accretion rate for 41 transects. The difference between the two studies attributes to the difference in shoreline stretch and time period; while Mary Divya Suganya et al. 2017 studied 59 km stretch for 38 years, this study calculated the change rate for 20.5 km stretch for 36 year time period.

Conclusions

Coringa Mangrove shoreline change analysis spanning 36 years from 1977 to 2013 enhanced by remote sensing, GIS and statistical analysis like End Point Rate, Net Shoreline Movement and Linear Regression Rates contributed a better understanding of the temporal and spatial rate of change of mangrove shoreline. Shoreline rate of change evaluated by the statistical methods EPR and LRR showed a strong correlation between the two. Quantitative estimates of shoreline changes reported the higher average accretion rate along the mangrove shoreline stretch throughout the period of four decades. About two-thirds of the mangrove shoreline accreted at the western side of the bay, while shoreline recession at the eastern side of the bottom of the bay was observed. The forcing mechanism of the mangrove shoreline migration was out of the scope of the present study and the work can extend these results using numerical modelling techniques.

Acknowledgements

Authors thank National Institute of Ocean Technology and National Center for Coastal Research, Chennai; Indian

National Centre for Ocean Information Services, Hyderabad; Landsat.org and M/s Kakinada Seaports Pvt. Ltd. for providing the required datasets. Authors acknowledge the encouragement received from Indian Maritime University in completing the work.

Disclosure statement

No potential conflict of interest was reported by the author(s).

Notes on contributors

Mrs. Garima Sharma is pursuing her PhD from Indian Maritime University, Visakhapatnam campus. She is working on morphological modeling for predicting long term evolution of Kakinada Bay. She completed M.Tech. in Environmental Engineering from MNIT Jaipur and also secured UGC-NET lectureship. She was awarded Child Scientist in 2004 under National Children's Science Congress, Guwahati.

Dr. K.V.K.R.K. Patnaik is working as Faculty at Indian Maritime University, Visakhapatnam campus. Main research interests include coastal processes, sediment dynamics and air-sea interaction studies. Currently two Ph.D. students are working under him. Successfully completed several Government sponsored research projects and guided several students for their M.Tech. Dissertations. Visited countries like Italy, Australia and Canada for advanced training and paper presentations.

References

Alemayehu F, Richard O, Kinyanjui MJ, Oliverv W. 2014. Assessment of shoreline changes in the period 1969-2010 in Watamu, Kenya. Global J Sci Frontier Res H Environ Earth Sci. 14(6):19–31.

Brooks SM, Spencer T. 2010. Temporal and spatial variations in recession rates and sediment release from soft rock cliffs, Suffolk coast, UK. Geomorphology. 124(1-2):26–41.

Chandramohan P, Jena BK, Sanil Kumar V. 2001. Littoral drift sources and sinks along the Indian coast. Curr Sci. 81(3):292–297.

Chandramohan P, Nayak BU. 1991. Long shore sediment transport along the Indian coast. Indian J Mar Sci. 20:110–114.

Cohen MCL, Lara RJ. 2003. Temporal changes of mangrove vegetation boundaries in Amazonia: application of GIS and remote sensing techniques. Wetl. Ecol. Manag. 11:223–231.

Cook PLM, Butler ECV, Eyre BD. 2004a. Carbon and nitrogen cycling on intertidal mudflats of a temperate Australian estuary. I. Benthic metabolism. Mar Ecol Prog Ser. 280:25–38.

Elnabwy MT, Elbeltagi E, El Banna MM, Elshikh MM, Motawa I, Kaloop MR. 2020. An Approach based on Landsat images for shoreline monitoring to support integrated coastal management—a case study, Ezbet Elborg, Nile Delta, Egypt. ISPRS Int J Geo-Inf. 9:199.

Fletcher CH, Romine BM, Genz AS, Barbee MM, Dyer M, Anderson TR, Lim SC, Vitousek S, Bochicchio C, Richmond BM. 2012. National assessment of shoreline change: Historical shoreline change in the Hawaiian Islands: U.S. Geological Survey Open-File Report 2011–1051, 55 p.

González-Villanueva R, Costas S, Pérez-Arlucea M, Jerez S, Trigo RM. 2013. Impact of atmospheric circulation patterns on coastal dune dynamics, NW Spain. Geomorphology. 185:96–109.

Hapke C, Kratzmann M, Himmelstoss E. 2013. Geomorphic and human influence on large-scale coastal change. Geomorphology. 199:160–170.

Jain S, Sridhar PN, Veera Narayan B, Surendran A. 2008. Morphodynamics of Godavari tidal inlets. In: Mohanty PK, editor. Monitoring and modelling lakes and coastal environments. Dordrecht: Springer; p. 237–243.

Jaya Kumar K. 2014. Remote sensing and GIS application in the management of Godavari mangrove wetland, AP, South India [Ph.D. thesis]. University of Madras.

Jickells TD, Rae JE, eds. 1997. Biogeochemistry of intertidal sediments, 9. Cambridge: Cambridge University Press.

Mary Divya Suganya G, Rajakumari S, Deepika B, Mahumitha R, Manonmani R, Thulasi Bai PD, Anantha Kamatchi G, Purvaja R, Ramesh R. 2017. Spatio temporal change analysis of mangroves along the Krishna and Godavari Deltaic region using IRS satellite images. User Interface Meet (UIM), Hyderabad, 2017.

Murty MR, Kumar CR, Reddy KM, Ramasubramanian R. 2011. Geospatial analysis of Coringa-Marine protected area, Andhra Pradesh, India. Int J Earth Sci Eng. 4 (8):24–38.

Nair S. 2017. Assessment and Vulnerability Modeling of Vanuatu's Mangroves using GIS and Remote Sensing. Master of Science Thesis, Central European University, Budapest.

Oyedotun TDT. 2014. Shoreline geometry: DSAS as a tool for historical trend analysis. Geomorphological techniques. Chapter 3(2.2). Br Soc Geomorphol. 1–12.

Pandey A, Nayak GN. 2013. Understanding distribution and abundance of metals with space and time in estuarine mudflat sedimentary environment. Environmental Earth Sciences. 70:2561–2575.

Reddy SC, Roy A. 2008. Assessment of three decade vegetation dynamics in mangroves of Godavari Delta, India using multi temporal satellite data and GIS. Res J Environ Sci. 2:108–115.

Reshma NK, Mani Murali R. 2018. Current status and decadal growth analysis of Krishna - Godavari delta regions using remote sensing. Journal of Coastal Research. Special Issue No. 85: Proceedings of the 15th International Coastal Symposium, Haeundae, Busan, 13–18 May 2018; pp. 1416–1420.

Sanders CJ, Smoak JM, Naidu AS, Araripe DR, Sanders LM, Patchineelam SR. 2010b. Organic carbon burial in a mangrove forest, margin and intertidal mud flat. Estuarine Coastal Shelf Sci. 90:168–172.

Satapathy DR, Krupadam RJ, Kumar LP, Wate SR. 2007. The application of satellite data for the quantification of mangrove loss and coastal management in the Godavari estuary, East coast of India. Environ Monit Assess. 134:453–469.

Satyanarayana B, Raman AV, Mohd-Lokman H, Dehairs F, Sharma VS, Dahdouh-Guebas Farid. 2009. Multivariate

methods distinguishing mangrove community structure of Coringa in the Godavari Delta, East coast of India. Aquatic Ecosyst Health Manag. 12(4):401–408.

Sheik M, Chandrasekar. 2011. A shoreline change analysis along the coast between Kanyakumari and Tuticorin, India, using digital shoreline analysis system. Geospatial Inf Sci. 14(4):282–293.

Thieler ER, Himmelstoss EA, Zichichi JL, Ergul A. 2009. Digital Shoreline Analysis System (DSAS) version 4.0 — An ArcGIS extension for calculating shoreline change: U.S. Geological Survey Open-File Report 2008-1278. *current version 4.3.

Thinh N, Hens L. 2017. A digital shoreline analysis system (DSAS) applied on mangrove shoreline changes along the Giao Thuy coastal area (Nam Dinh, Vietnam) during 2005-2014. Vietnam J Earth Sci. 39:87–96.

Tran TV, Nguyen H, Xuan A, Dahdouh-Guebas F, Koedam N. 2013. Application of remote sensing and GIS for detection of long-term mangrove shoreline changes in Ca Mau, Vietnam. Biogeosci Discuss. 10:20047–20077.